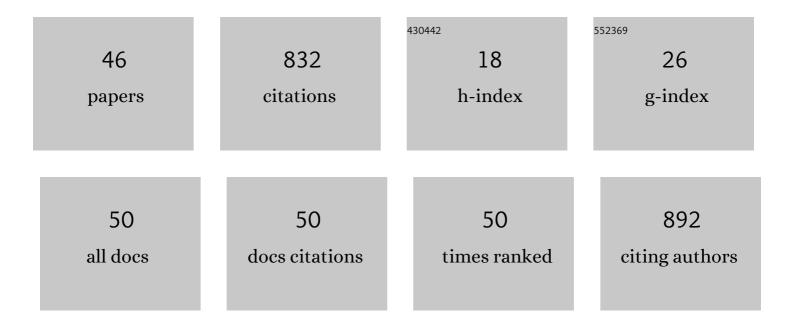
## Adnane Osmane

List of Publications by Year in descending order

Source: https://exaly.com/author-pdf/8404678/publications.pdf Version: 2024-02-01



#	Article	IF	CITATIONS
1	Electron Energy Partition across Interplanetary Shocks. I. Methodology and Data Product. Astrophysical Journal, Supplement Series, 2019, 243, 8.	3.0	57
2	Relativistic Electrons Produced by Foreshock Disturbances Observed Upstream of Earth's Bow Shock. Physical Review Letters, 2016, 117, 215101.	2.9	55
3	Autogenous and efficient acceleration of energetic ions upstream of Earth's bow shock. Nature, 2018, 561, 206-210.	13.7	47
4	A statistical study of the dawnâ€dusk asymmetry of ion temperature anisotropy and mirror mode occurrence in the terrestrial dayside magnetosheath using THEMIS data. Journal of Geophysical Research: Space Physics, 2015, 120, 5489-5503.	0.8	45
5	Electron Energy Partition across Interplanetary Shocks. II. Statistics. Astrophysical Journal, Supplement Series, 2019, 245, 24.	3.0	40
6	Solar Wind Properties and Geospace Impact of Coronal Mass Ejectionâ€Đriven Sheath Regions: Variation and Driver Dependence. Space Weather, 2019, 17, 1257-1280.	1.3	35
7	A statistical study into the spatial distribution and dawnâ€dusk asymmetry of dayside magnetosheath ion temperatures as a function of upstream solar wind conditions. Journal of Geophysical Research: Space Physics, 2015, 120, 2767-2782.	0.8	34
8	Influence of velocity fluctuations on the Kelvinâ€Helmholtz instability and its associated mass transport. Journal of Geophysical Research: Space Physics, 2017, 122, 9489-9512.	0.8	28
9	The impact of solar wind ULF <i>B</i> <sub><i>z</i></sub> fluctuations on geomagnetic activity for viscous timescales during strongly northward and southward IMF. Journal of Geophysical Research: Space Physics, 2015, 120, 9307-9322.	0.8	26
10	Statistical analysis of mirror mode waves in sheath regions driven by interplanetary coronal mass ejection. Annales Geophysicae, 2018, 36, 793-808.	0.6	24
11	Magnetosheath control of solar windâ€magnetosphere coupling efficiency. Journal of Geophysical Research: Space Physics, 2016, 121, 8728-8739.	0.8	23
12	FORESAILâ€1 CubeSat Mission to Measure Radiation Belt Losses and Demonstrate Deorbiting. Journal of Geophysical Research: Space Physics, 2019, 124, 5783-5799.	0.8	23
13	ON THE CONNECTION BETWEEN MICROBURSTS AND NONLINEAR ELECTRONIC STRUCTURES IN PLANETARY RADIATION BELTS. Astrophysical Journal, 2016, 816, 51.	1.6	22
14	Universal properties of mirror mode turbulence in the Earth's magnetosheath. Geophysical Research Letters, 2015, 42, 3085-3092.	1.5	21
15	Energetic electron acceleration observed by MMS in the vicinity of an Xâ€line crossing. Geophysical Research Letters, 2016, 43, 7356-7363.	1.5	21
16	Electron Energy Partition across Interplanetary Shocks. III. Analysis. Astrophysical Journal, 2020, 893, 22.	1.6	21
17	Magnetic field fluctuation properties of coronal mass ejection-driven sheath regions in the near-Earth solar wind. Annales Geophysicae, 2020, 38, 999-1017.	0.6	21
18	Radial Evolution of Magnetic Field Fluctuations in an Interplanetary Coronal Mass Ejection Sheath. Astrophysical Journal, 2020, 893, 110.	1.6	19

Adnane Osmane

#	Article	IF	CITATIONS
19	Formation of Foreshock Transients and Associated Secondary Shocks. Astrophysical Journal, 2020, 901, 73.	1.6	18
20	Statistical Analysis of Magnetic Field Fluctuations in Coronal Mass Ejection-Driven Sheath Regions. Frontiers in Astronomy and Space Sciences, 2021, 7, .	1.1	17
21	Outer radiation belt and inner magnetospheric response to sheath regions of coronal mass ejections: a statistical analysis. Annales Geophysicae, 2020, 38, 683-701.	0.6	17
22	Magnetosheath jet evolution as a function of lifetime: global hybrid-Vlasov simulations compared to MMS observations. Annales Geophysicae, 2021, 39, 289-308.	0.6	15
23	Outer Van Allen Radiation Belt Response to Interacting Interplanetary Coronal Mass Ejections. Journal of Geophysical Research: Space Physics, 2019, 124, 1927-1947.	0.8	14
24	Compacting the description of a time-dependent multivariable system and its multivariable driver by reducing the state vectors to aggregate scalars: the Earth's solar-wind-driven magnetosphere. Nonlinear Processes in Geophysics, 2019, 26, 429-443.	0.6	14
25	Cross Helicity of the 2018 November Magnetic Cloud Observed by the Parker Solar Probe. Astrophysical Journal Letters, 2020, 900, L32.	3.0	14
26	On the generation of proton beams in fast solar wind in the presence of obliquely propagating Alfvén waves. Journal of Geophysical Research, 2010, 115, .	3.3	13
27	Statistical mapping of ULF Pc3 velocity fluctuations in the Earth's dayside magnetosheath as a function of solar wind conditions. Advances in Space Research, 2016, 58, 196-207.	1.2	13
28	Dynamical-systems approach to relativistic nonlinear wave-particle interaction in collisionless plasmas. Physical Review E, 2012, 85, 056410.	0.8	11
29	Relativistic surfatron process for Landau resonant electrons in radiation belts. Nonlinear Processes in Geophysics, 2014, 21, 115-125.	0.6	11
30	Hybrid-Vlasov modelling of nightside auroral proton precipitation during southward interplanetary magnetic field conditions. Annales Geophysicae, 2019, 37, 791-806.	0.6	11
31	Jensen‧hannon Complexity and Permutation Entropy Analysis of Geomagnetic Auroral Currents. Journal of Geophysical Research: Space Physics, 2019, 124, 2541-2551.	0.8	11
32	The dawn–dusk asymmetry of ion density in the dayside magnetosheath and its annual variability measured by THEMIS. Annales Geophysicae, 2016, 34, 511-528.	0.6	10
33	Temperature variations in the dayside magnetosheath and their dependence on ionâ€scale magnetic structures: THEMIS statistics and measurements by MMS. Journal of Geophysical Research: Space Physics, 2017, 122, 6165-6184.	0.8	10
34	Solar wind energy input to the magnetosheath and at the magnetopause. Geophysical Research Letters, 2015, 42, 4723-4730.	1.5	9
35	On the threshold energization of radiation belt electrons by double layers. Journal of Geophysical Research: Space Physics, 2014, 119, 8243-8248.	0.8	8
36	Resolution dependence of magnetosheath waves in global hybrid-Vlasov simulations. Annales Geophysicae, 2020, 38, 1283-1298.	0.6	7

Adnane Osmane

#	Article	IF	CITATIONS
37	Quantifying the non-linear dependence of energetic electron fluxes in the Earth's radiation belts with radial diffusion drivers. Annales Geophysicae, 2022, 40, 37-53.	0.6	7
38	Cross helicity of interplanetary coronal mass ejections at 1Âau. Monthly Notices of the Royal Astronomical Society, 2022, 514, 2425-2433.	1.6	7
39	Subcritical Growth of Electron Phase-space Holes in Planetary Radiation Belts. Astrophysical Journal, 2017, 846, 83.	1.6	6
40	Radial Diffusion of Planetary Radiation Belts' Particles by Fluctuations with Finite Correlation Time. Astrophysical Journal, 2021, 912, 142.	1.6	5
41	Outer Van Allen belt trapped and precipitating electron flux responses to two interplanetary magnetic clouds of opposite polarity. Annales Geophysicae, 2020, 38, 931-951.	0.6	4
42	The impact on global magnetohydrodynamic simulations from varying initialisation methods: results from GUMICS-4. Annales Geophysicae, 2017, 35, 907-922.	0.6	3
43	Structure and fluctuations of a slow ICME sheath observed at 0.5 au by the Parker Solar Probe. Astronomy and Astrophysics, 2022, 663, A108.	2.1	3
44	Cosmic noise absorption signature of particle precipitation during interplanetary coronal mass ejection sheaths and ejecta. Annales Geophysicae, 2020, 38, 557-574.	0.6	2
45	Phase Space Density Analysis of Outer Radiation Belt Electron Energization and Loss During Geoeffective and Nongeoeffective Sheath Regions. Journal of Geophysical Research: Space Physics, 2022, 127, .	0.8	2
46	Estimating Inner Magnetospheric Radial Diffusion Using a Hybrid-Vlasov Simulation. Frontiers in Astronomy and Space Sciences, 2022, 9, .	1.1	2